3.1 THERMO-RADIATIVE MODELING AND ENERGY BALANCE OF THE URBAN CANOPY : RELATIONS BETWEEN SIMULATED AND MEASURABLE TEMPERATURES

Aurélien Hénon*, Patrice Mestayer, Dominique Groleau
Laboratoire de Mécanique des Fluides, Institut de Recherche en Sciences et Techniques de la Ville, CNRS, Ecole Centrale de Nantes, France

1. INTRODUCTION

When studying an urban fragment (~ 10^4 m^2), the presence of horizontal (ground and vegetation), vertical (walls) and oblique (roofs) elements implies complex descriptions of the 3D model and of the associated temperatures.
Parametrical relations between the different “surface temperatures” (physical temperature, aero-dynamical temperature, radiative temperature) must take into account the geometrical features of the urban fragment and the micro-meteorological conditions. To construct these relationships, numerical simulations are carried out with micro-scale thermo-radiative and aerothermodynamical transfer models. The software SOLENE simulates the air-solid thermo-radiative transfers with fine meshes and the restitution of the visible and thermal infrared radiative fluxes towards the sky or a virtual sensor (Ringenbach, 2004). Parameterizations of heat exchange through walls are also introduced, with several layers (Vinet, 2000). The basic configurations of our urban fragment simulations reproduce the sites where experimental data files were obtained during two intensive observation periods of UBL-ESCOMPTE, in Marseilles (Mestayer et al., 2005), and CAPITOUL, in Toulouse (Masson et al., 2004). After computation of the simulated physical surface temperatures, virtual TIR sensors are introduced to evaluate the radiant temperature of the observed walls, with various types of sensor configuration: airborne or satellite, in oblique or vertical sighting. Then, infrared measurements from these virtual sensors are compared with the different calculated energy flows. The present results are the first step of a study, whose final aim is to evaluate the heat fluxes from currently operational infrared very high resolution remote sensors, e.g., to correlate the sensible heat flux to the infrared values measured from satellites.

2. The thermo-radiative model : SOLENE

The model SOLENE allows to simulate the thermo-radiative behavior of a three dimensional urban fragment, in transitory regime.

* *Corresponding author address :* Aurélien Hénon, Ecole Centrale de Nantes, Laboratoire de Mécanique des Fluides, 1 rue de la Noë, BP 92101, 44321 Nantes CEDEX3, FRANCE;
e-mail : aurelien.henon@ec-nantes.fr

2.1 *Description of the model*

The surface studied in that case is an urban fragment of 10 000 m ². The envelope of this fragment is divided into 17000 triangular meshes (Fig. 1) of variable dimensions (metric facets). A 1024 mesh hemispherical sky vault closes the scene.

For each time step, at every facet of the mesh grid, an energy balance is computed, between the energy fluxes of direct and diffuse short wave radiations (solar flux), infrared radiations from walls and atmosphere, sensible heat due to convective transfers between walls and atmosphere, and to conduction inside the walls. This last flux is computed with a multi-layer wall thermal model (Fig. 2), where the conductive transfers introduce heat storage in order to reconstruct the inertial role of walls.

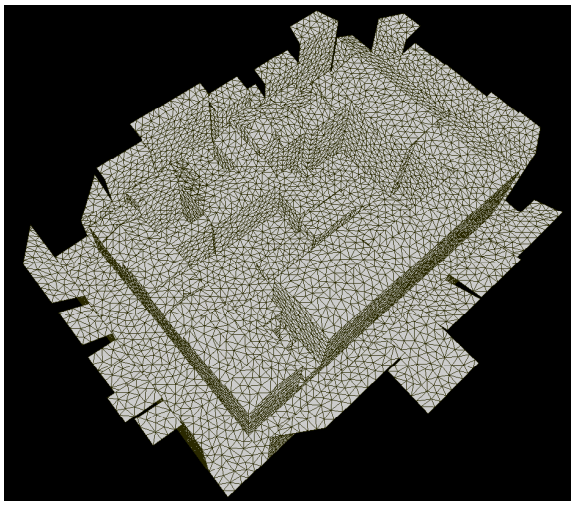

Fig. 1. View of the modeled urban fragment

Each mesh is attributed its own set of wall characteristics, depending on the materials and thickness of the layers.

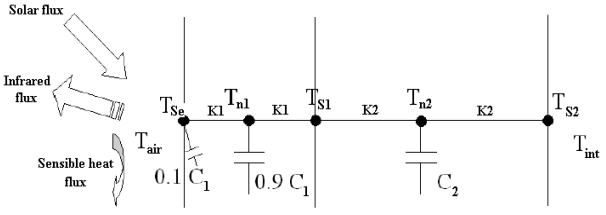

Fig. 2. Multilayer wall thermal modeling schema

During the thermo-radiative simulation, geometrical effects such as solar position, shadowing, radiation multiple reflections are taken into account.

2.2 *Application*

The simulations that are presented here correspond to the Intensive Observation Period 2b of the UBL-ESCOMPTE series of measurements, held in Marseilles (Mestayer et al., 2005). An urban fragment, chosen for being very representative of the regular, periodical city center urban fabric, has been modeled.
The parameterization is based on the data obtained during the series of measurements: air temperature, wind speed, direct solar flux, diffused solar flux, incoming infrared flux at a nearby meteorological mast (Lagouarde et al., 2004).
The simulations have been carried out for a 3 days period, with a 15 minutes time step. Only the results of the third day (June 26th, 2001) are used, so that thermal inertia effects are included.

3. Results and discussion

3.1 *Integral fluxes of the whole fragment*

One model output is, at each time step, and for each facet, the temperature of the wall surface (Fig. 3). These temperatures allow to determine both the sensible heat flux towards the atmosphere and the infrared flux towards the sky, integrated for the whole urban fragment.

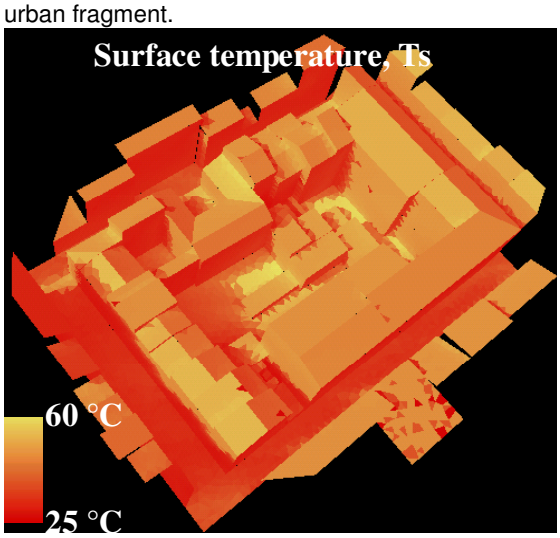

Fig. 3. Distribution of surface temperature, at 16:00 (local solar time)

The diurnal cycle (local solar time) of these two fluxes is traced on Fig.4. The results from a virtual remote sensor appearing in Fig.4b will be commented in the next section. The measurements of the real remote sensor, placed on the central site mast located close to the simulated scene, are represented on the same graphs. The sensible heat flux results from the model seem in good agreement with the measurements. As for the infrared radiation, it is difficult to compare precisely the modeled flux, corresponding to the sum of the infrared emissions towards the whole sky vault, with the measured flux, corresponding to the only infrared radiation that has reached the sensor which depends highly on the position of the sensor, i.e. its height, its orientation, and the "landscape" it observes.

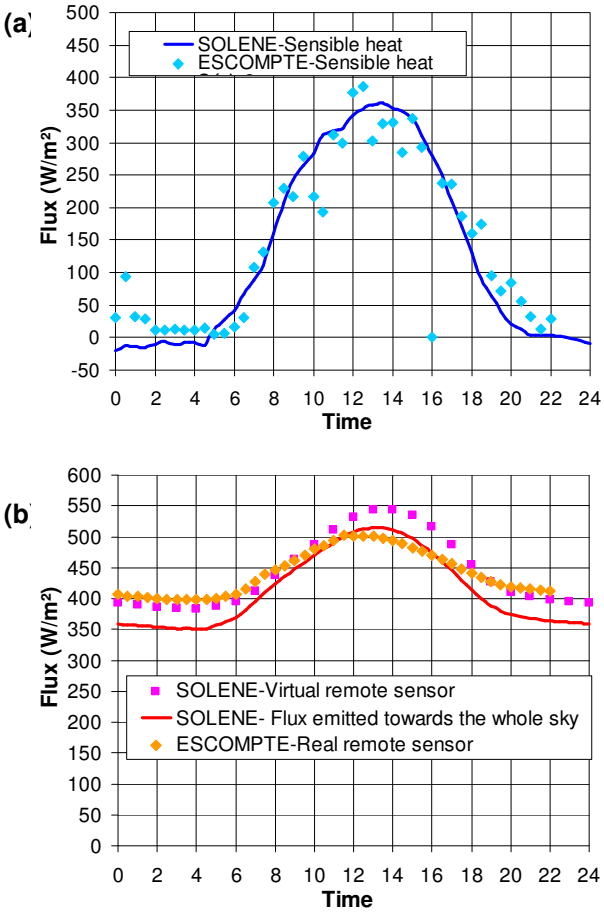

Fig. 4. Sensible heat (a) and infrared (b) flux variations

That is the reason it has been decided to determine the modeled infrared flux by a virtual remote sensor, that can be placed anywhere above the scene.

3.2 *Virtual remote sensors in vertical sighting*

Virtual sensors are placed in various locations, above the urban fragment (Fig. 5) at 30 and 50 m above ground level (agl).
Two of them are placed just above the center of the scene, mainly composed of an inner courtyard. These sensors correspond to vertical sighting.
The other sensors are placed above the roofs as well, in the middle of each of the four sides of the scene. These sensors carry out measurements corresponding to various zenithal and azimuthal orientations; e.g. sensor W50, placed above the western side at 50 m agl, corresponds to an eastward viewing with an average zenithal angle of 37° with the vertical.

Moreover, associating sensors –i.e., summing their measurements- makes it possible to obtain a "new"' sensor in vertical sighting (assuming the urban fabric is periodical); e.g., the association of sensors W50 and E50, located on opposite sides, enables obtaining an equivalent vertical sighting sensor, placed at 50 m agl above the roofs of a North-South oriented street.

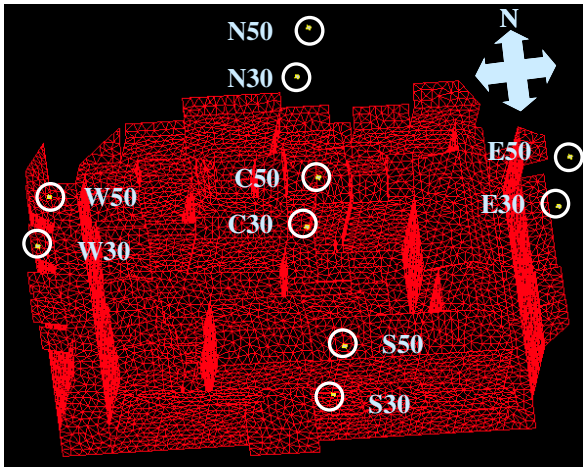

Fig. 5. Location and designation of the used virtual remote sensors

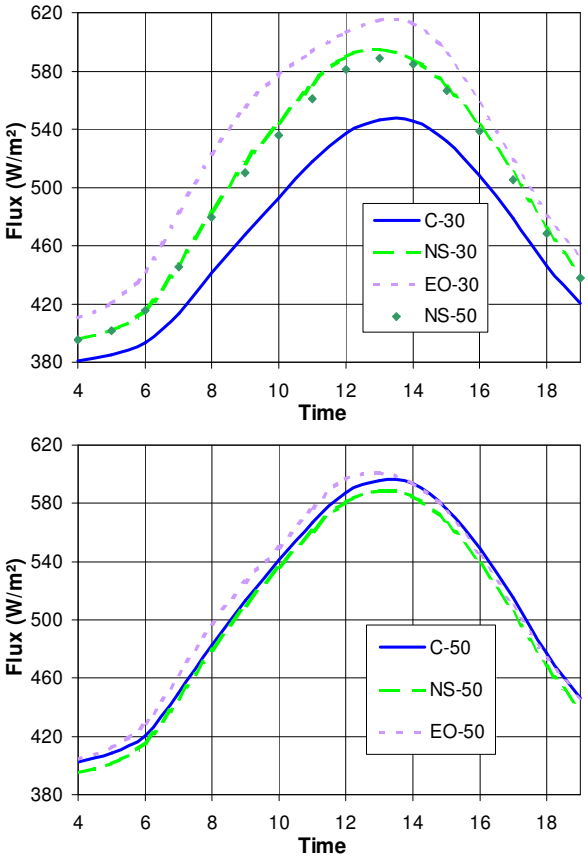

Fig. 6. Variation of virtual remote sensor measurements, for different vertical sighting configurations

Fig. 6 gathers measurements from virtual sensors corresponding to several vertical sighting configurations. The curves have been separated in two groups, for the 30-m high sensors, and for the 50-m high ones.
It appears that the measurements are much more sensitive to the sensor position at 30 m than 50 m, due to the larger influence of the close environment. Here, at 50 m the sensors seem to be sufficiently high to account for a "general" viewing of the scene.

3.3 *Directional virtual sensors*

Now, we study infrared measurements by a directional virtual sensor. It is possible to see this sensor as one of the previous ones which would have been moved away from the scene in a chosen direction, at a distance tending towards infinity.
The direction of this measurement is defined by its zenithal and azimuthal angles, so it is possible to represent the infrared measurement, at a given time, for the whole possible directions, by drawing a directional "rosette" (Fig. 7). The central point corresponds to the vertical sighting: in that case, the measurement disregards the vertical walls, unlike the sensors that are placed at a limited height. Thanks to the rosette, it is possible to observe, at any instant, the variability of the measurement as a function of the direction.

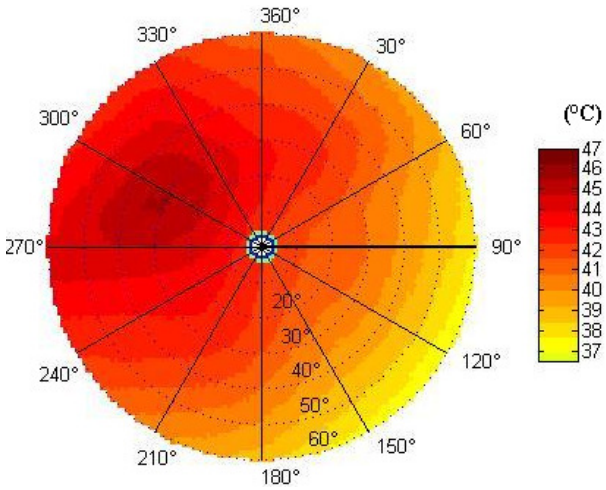

Fig. 7. Angular variations of radiant temperature, measured by a directional virtual sensor

Curves have been drawn for the whole day, for different sensor configurations. Fig. 8 corresponds to northward and southward, directional and conventional sensors at a 42° zenithal angle with the vertical. Fig. 9 represents as well the values worked out by eastward and westward sensors.
For the two southward oriented sensors (N30(180;42) and Directional(180;42)), the measurements from the directional sensor and from the 30-m high sensor are in phase and generally equal.

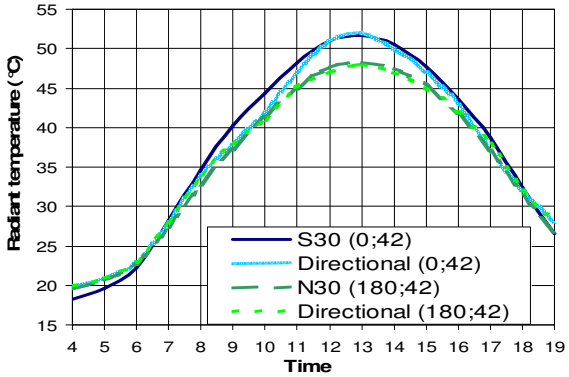

Fig. 8. Variation of directional and conventional measurements, for northward and southward oriented virtual sensors

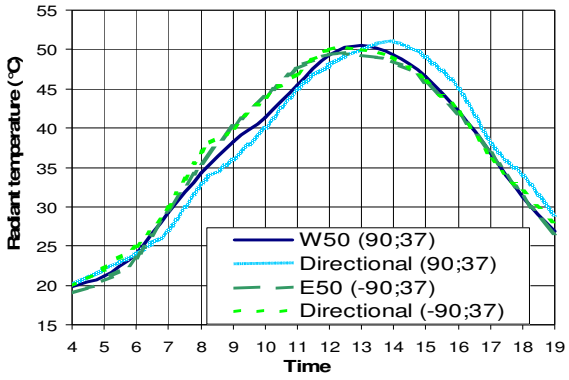

Fig. 9. Same as Fig.8 for eastward and westward oriented virtual sensors

As for the northward sensors, measurements are also in phase, but a significant difference appears during the morning. This can be explained by the fact that the directional sensor takes into account the North-South oriented streets, contrary to the 30-m high sensor, for which they are hidden. Indeed, these streets are clearly colder than the southward oriented roofs during the morning, because the sun does not directly light them then. On the other hand, around midday these streets are directly lit, which makes it possible for them to make up the temperature difference with the roofs, and to reduce the difference between the measurements of the two sensors.

For the westward oriented sensors (Fig.9), the curves match each other quite well. Nonetheless, for the eastward oriented sensors, the phase difference between the directional and conventional sensor curves seems important. The lag of the directional sensor is logical because it mainly measures the fluxes coming from the westward oriented facets, lit from the beginning of the afternoon but warmed up later than the other facets. However, the measurements from the 50-m high sensor show very little phase difference compared to the measurements from the opposite side. We can suppose that, due to its positioning, it widely takes account of facets which are not westward oriented.

So, in the studied case, for the eastward oriented sensors, the directional effects are much more important for a directional sensor than for a sensor that is placed just above the scene. Nevertheless, for the other directions, the measurements from the different sensors seem in phase.

Moreover, in the morning, during the temperature rise, some differences may be observed between the different measurements: this is probably due to the proximity of the obstacles in the field of vision of the sensors that are close to the scene. However, these differences are rather small in the afternoon, during the surface temperature drop.

4. Conclusion

We have underscored the strong variations of the infrared measurements, in terms of phase and amplitude, as a function of the remote sensor position and orientation (reaching several dozens of $W.m^{-2}$ at a given time for the same urban fragment). This can justify the differences observed between the distinctly placed real and virtual sensors in Fig. 4b.

We will complement this remote sensor sensibility study with further simulations, introducing various urban fabric types (aspect ratio, different materials, non perpendicular streets).

For each urban configuration, we will choose the most adapted sensor parameterization (height agl, azimuthal and zenithal orientations, close environment composition and geometry) to determine the infrared flux emitted towards the sky and will correlate it to the corresponding sensible heat flux. This last flux will be expressed in terms of mean equivalent convective transfer temperature, in order to enable the comparison with the selected infrared remote sensor brightness temperature.

5. References

Lagouarde, J.-P., Moreau, P., Irvine, M., Bonnefond, J.-M., Voogt, J., and Solliec, F.: 2004, Airborne Experimental Measurements of the Angular Variations in Surface Temperature over Urban Areas: Case Study of Marseille (France). *Remote Sens. Environ.*, **93**, 443–462.

Masson, V., Pigeon, G., Durand, P., Gomes, L., Salmond, J., Lagouarde, J.-P., Voogt, J., Oke, T., Lac, C., Liousse, C., Maro, D., 2004: The Canopy and Aerosol Particles InTOulouse Urban Layer (CAPITOUL) experiments: first results. In AMS Editions, editor, *PROCEEDINGS of the Fifth Symposium on the Urban Environment*, 23-27Aug.

Mestayer, P.G., P. Durand *et alii*, 2005: The Urban Boundary Layer Field Campaign in Marseille (UBL/CLU-ESCOMPTE): Set-up and First Results. *Boundary-Layer Meteorology*, **114**, 315-365.

Ringenbach, N., 2004: Radiative balance and heat flow in urban climatology : measurements, modeling and validation for Strasbourg, 85-99.

Vinet, J., 2000: Contribution to thermo-aerodynamical modeling of the urban microclimate. Characterization of the impact of water and vegetation on the conditions of comfort in external spaces, 149-152.